Click Here for Full Article

Paleomagnetism of the Santa Fé Group, central Brazil: Implications for the late Paleozoic apparent polar wander path for South America

Daniele Brandt,[1] Marcia Ernesto,[1] Antonio Carlos Rocha-Campos,[2] and Paulo Roberto dos Santos[2]

[1] Paleomagnetic and rockmagnetic data are reported for the Floresta Formation (Santa Fé Group) of the Sanfranciscana Basin, central Brazil. This formation represents the Permo-Carboniferous glacial record of the basin and comprises the Brocotó (diamictites and flow diamictites), Brejo do Arroz (red sandstones and shales with dropstones and invertebrate trails), and Lavado (red sandstones) members, which crop out near the cities of Santa Fé de Minas and Canabrava, Minas Gerais State. Both Brejo do Arroz and Lavado members were sampled in the vicinities of the two localities. Alternating field and thermal demagnetizations of 268 samples from 76 sites revealed reversed components of magnetization in all samples in accordance with the Permo-Carboniferous Reversed Superchron. The magnetic carriers are magnetite and hematite with both minerals exhibiting the same magnetization component, suggesting a primary origin for the remanence. We use the high-quality paleomagnetic pole for the Santa Fé Group (330.9°E 65.7°S; N = 60; α_{95} = 4.1°; k = 21) in a revised late Carboniferous to early Triassic apparent polar wander path for South America. On the basis of this result it is shown that an early Permian Pangea A-type fit is possible if better determined paleomagnetic poles become available.

1. Introduction

[2] The Paleozoic APWP for South America is mainly based on paleomagnetic data from sedimentary rocks which are generally deficient in good geochronological control. Most of these rocks have hematite as the main magnetic carrier. The origin and age of this mineral remain largely unknown hampering the proper interpretation of the time of magnetization acquisition. Uncertainty increases for paleomagnetic data from sampling areas that underwent tectonic deformation as restoration of magnetization vectors to the prefolding position sometimes may lead to spurious results [*Stewart*, 1995; *Pueyo et al.*, 2003]. Fold tests are generally performed assuming a horizontal strike line, and this is not always the case as already demonstrated [*MacDonald*, 1980]. Unfortunately, magmatism during Late Paleozoic was not widespread over the South American plate limiting the number of trustworthy paleomagnetic data from well-dated igneous rocks.

[3] In the last two decades new analytical facilities have become available for rock magnetism studies coupled with paleomagnetic investigations. Furthermore, the knowledge

about the behavior of the geomagnetic field has also improved greatly. As a consequence, selection of reliable paleomagnetic poles must be more rigorous [e.g., *Van der Voo*, 1990; *McElhinny et al.*, 2003]. There are few poles from stable areas of South America, most of which rank poorly in quality assessments. As an example, the Carboniferous Taiguati pole [*Creer*, 1970] is still being used by some authors for lack of a better alternative, even though this pole is based only on the natural remanent magnetization.

[4] These problems are the cause of the considerable dispersion in the assumedly coeval paleomagnetic poles. This dispersion means that proposed APWPs for the middle-late Carboniferous to early Triassic of South America [e.g., *Rapalini et al.*, 1994; *McElhinny and McFadden*, 2000; *Gilder et al.*, 2003; *Tomezzoli et al.*, 2006] still require substantiation. The ongoing discussion over whether the eastern Australia Late Carboniferous poles are representative of the rest of the continent [*Briden and McElhinny*, 2004] means that this problem cannot be resolved by simply using paleomagnetic data from other parts of Gondwana. One consequence of this continued uncertainty is the persistent controversy over the Pangea reconstructions, in which the position of Gondwana remains dubious [*Van der Voo and Torsvik*, 2001; *Muttoni et al.*, 2003]. Depending on the considered paleomagnetic poles northwestern South America is placed against the southern edge (classical Wegnerian Pangea A) or alternatively the eastern coast (Pangea B; see

---

[1]Department of Geophysics, University of São Paulo, São Paulo, Brazil.
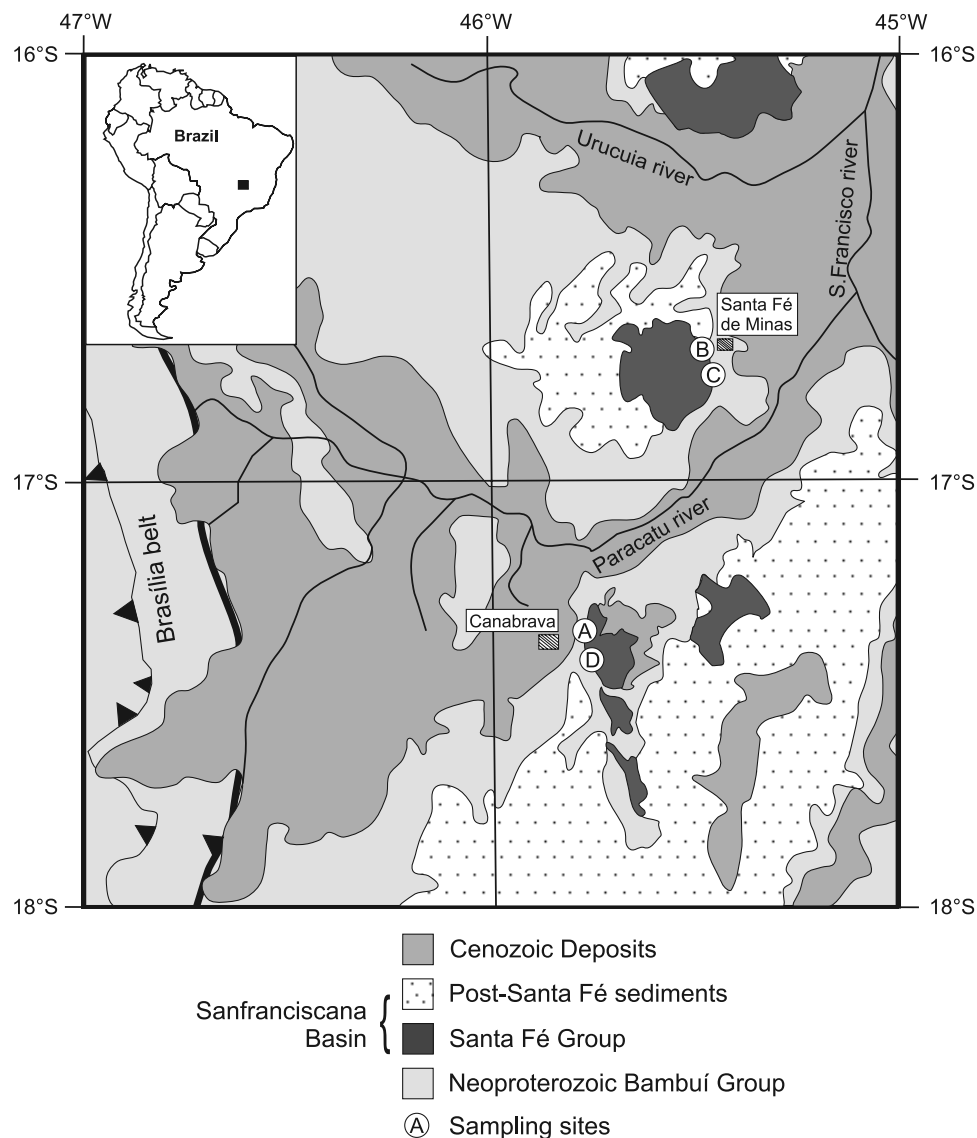[2]Institute of Geosciences, University of São Paulo, São Paulo, Brazil.

Figure 1. Simplified geological map (based on that from *Schobbenhaus et al.* [2004]) of the Sanfranciscana Basin indicating the sampling site locations of the Brejo do Arroz member (A and B), Lavado member (C and D), and the local basement (Bambuí Group, site A).

Morel and Irving [1981]) of North America during early Permian to Permo-Triassic. However, the alternative model has been criticized by some authors [e.g., *Weil et al.*, 2001] as the large relative displacement of Gondwana from position B back to the classical reconstruction just prior to the continental breakup in the early Jurassic would produce geological structures which are not evident. The aim of this paper is to provide a new reference paleomagnetic pole for the Permo-Carboniferous of South America, and to discuss the implications for the APWP for this continent.

2. Geological Setting

[5] The Santa Fé Group (SFG) corresponds to the Late Paleozoic deposits of the sedimentary Sanfranciscana Basin (Figure 1) in the São Francisco Craton, central Brazil [*Campos and Dardenne*, 1994, 1997a]. The basin area is about 1100 km long and 200 km wide, with elongation in the N-S direction, but formerly occupied a much larger area [*Campos and Dardenne*, 1997b]. The SFG rests discordantly over the glacially striated pavements of the Neoproterozoic rocks of the Três Marias Formation (Bambuí Group), and was preserved in paleodepressions [*Campos and Dardenne*, 1997b]. The SFG comprises the Floresta and Tabuleiro formations. The former represents the glacial record of the basin, and comprises the Brocotó (diamictites and flow diamictites), Brejo do Arroz (red shales and sandstones with dropstones and invertebrate trails), and Lavado (red sandstones) members, which interfinger laterally. Association with striated pavements and dropstones as well as presence of striated clasts supports interpretation of the diamictites as of glacial origin. The Lavado member (LM) is described as being originated by a fluvioglacial system of braided type. The Tabuleiro Fm. is constituted by aeolian sandstones, and is unconformably covered by the Cretaceous Areado Group.
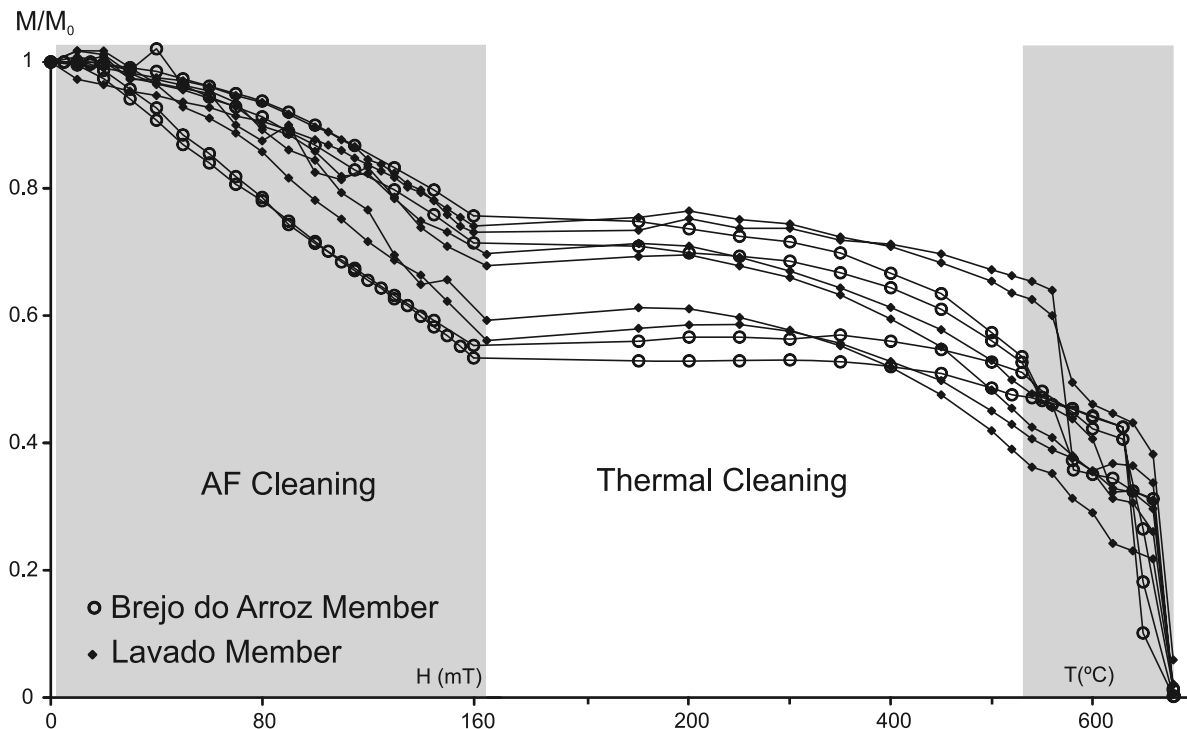
Figure 2. Magnetization intensity variation curves during AF and thermal cleaning. Open circles correspond to BAM samples, and closed diamonds correspond to the LM samples.

[6] According to *Campos and Dardenne* [1994] the thickness of the entire SFG succession does not exceed 250 m given the limited subsidence of the basin. These authors also noted limited effects of elevated pressure and temperature in SFG; the sandstones of the Lavado member preserve primary porosity that is only partially infilled by carbonatic cement. Those authors found up to 5% of oxides (magnetite, hematite and ilmenite) in the Lavado member, and attributed the red color of the rocks to the oxide films enveloping the detrital grains.

[7] The Permo-Carboniferous age of the SFG was proposed by *Campos and Dardenne* [1994] on the basis of correlations between the glacial facies and characteristics icnofossils of the Santa Fé Group and those found within the glacial Itararé Subgroup of the Paraná Basin (southern Brazil). The age of the Itararé Subgroup is believed to be within the range of late Carboniferous (Westphalian) to early Permian (Sakmarian) on the basis of biostratigraphic data [*Daemon and Quadros*, 1970; *Souza et al.*, 2003]. Some attempts to provide absolute radiometric ages to the late Paleozoic rocks of the Paraná Basin reached relative success. U-Pb SHRIMP data from zircons found in ashfall deposits in the Floresta Formation and the lower part of the Itararé Group gave ages of 359.6 ± 8.1 Ma and 356.9 ± 22 Ma [*Rocha-Campos et al.*, 2006], respectively which the authors considered too old in view of the stratigraphic and biostratigraphic control. In the Paraná Basin the post-Itararé Rio Bonito Formation gave ages in the interval 299 to 267 Ma [*Guerra-Sommer et al.*, 2006; *Rocha-Campos et al.*, 2006; *Matos et al.*, 2001], with peak age around 298 Ma. As a consequence, this result should be seen as a minimum age for the Itararé Group, and eventually for the Santa Fé Group.

However, it may conflict with the widely accepted intercontinental biostratigraphic correlations [*Iannuzzi*, 2008].

3. Paleomagnetism

[8] The paleomagnetic sampling was performed in four sections of the Floresta Formation cropping out near the cities of Canabrava and Santa Fé de Minas (Figure 1), northwest of Minas Gerais State which are about 100 km apart. Two of the sections correspond to the BAM (sections A and B), and are about 0.6 and 8 m thick (5 and 6 stratigraphic levels respectively). The Brejo do Arroz shales are horizontally layered, and E-W dips not exceeding 2–3° were measured in the BAM sandstones (section A). Three dropstones (10–20 cm clasts of metapelites) in Brejo do Arroz sections were also sampled. The other two sections are from the LM (section C, 47 levels; section D, 18 levels), each one ∼10 m thick. Throughout this work section C will be presented as two complementary subsections C1 and C2 as they were sampled in different parts of the outcrop, and relative positions could not be established precisely. Sampling also included 10 stratigraphic levels of the basement (Bambuí Group) occurring near section A (Figure 1) of the BAM, comprising a vertical section of about 3.5 m. These layers dip about 15° to SW.

[9] Standard paleomagnetic cores were collected using a gasoline powered drill and oriented using both magnetic and solar compasses whenever possible. In the laboratory, 604 specimens (one inch diameter and 2.2 cm long) were prepared from 243 cores and 25 oriented hand samples. Specimens were stored in a magnetically shielded room in the Laboratory of Paleomagnetism, University of São Paulo,
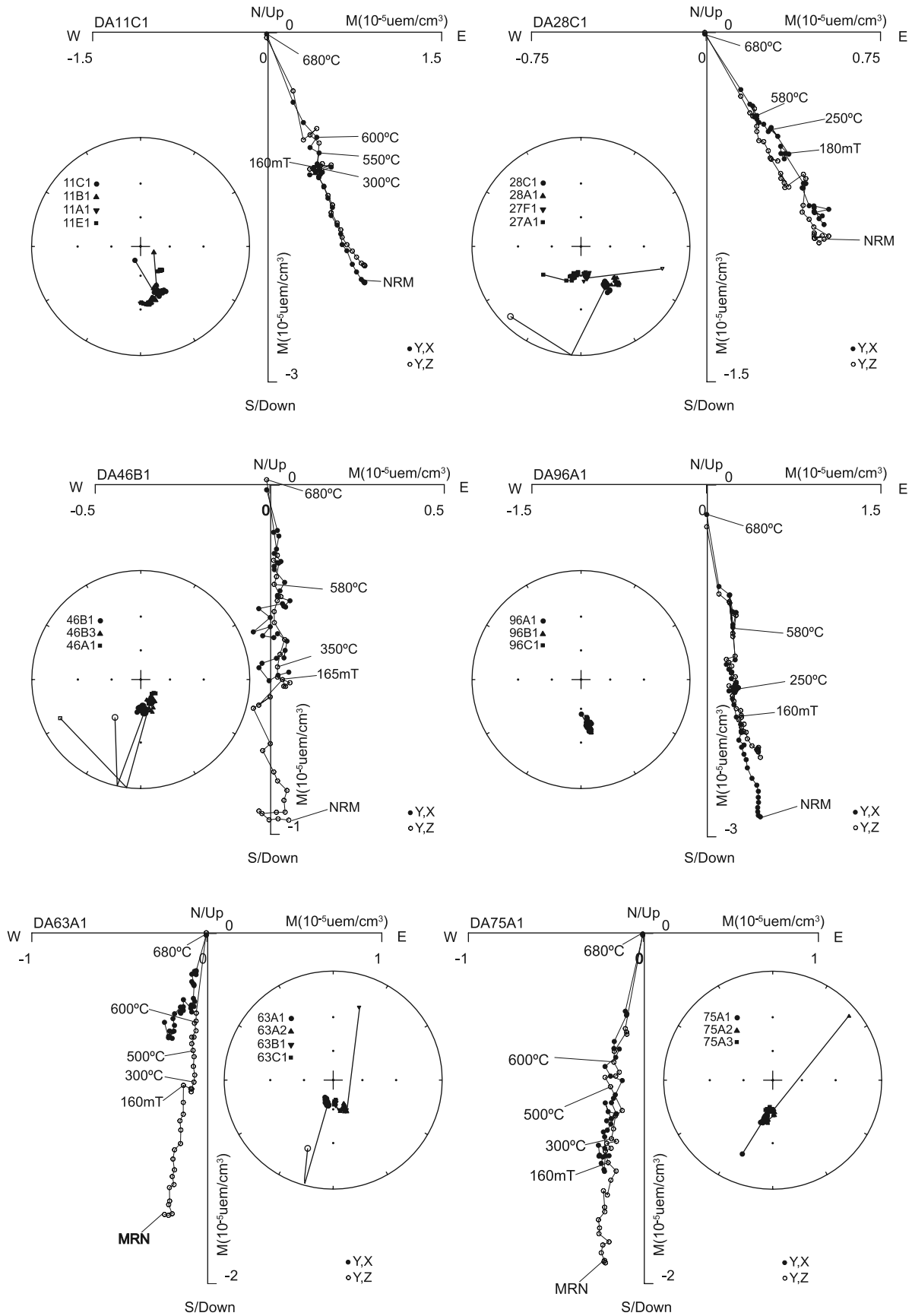
Figure 3. Examples of gradual demagnetization of Santa Fé samples on stereo and orthogonal plots. Behavior of sister samples are shown on stereo diagrams. Open (solid) symbols are negative (positive) inclinations or vertical (horizontal) projections.
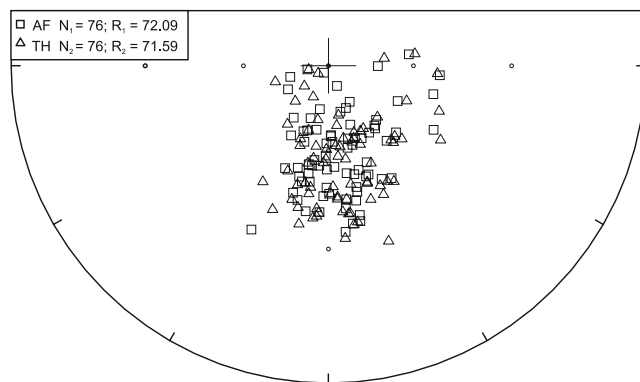
Figure 4. Stereo plot of magnetization components from the same samples obtained after AF (squares) and thermal (triangles) demagnetizations. All directions have positive inclinations.

where all demagnetization routines were performed. We used an AF demagnetizer coupled to the 2G Enterprises cryogenic magnetometer with peak applied fields of 160 mT reached in 24 steps. Thermal demagnetization up to 680°C was carried out in a MMTD60 furnace, and remanences were measured in the cryogenic magnetometer. Susceptibility variations were controlled by means of a Bartington susceptometer after each heating step.

[10] At the end of the AF process, all pilot specimens (140 samples) retained at least 50% of the remanence (Figure 2), which was partially removed at temperatures above 550°C, and completely erased by 680°C. Another 40 specimens were submitted to only thermal demagnetization. The characteristic remanent magnetization (ChRM) components were calculated by principal component analysis [*Kirschvink*, 1980], and the means were evaluated using *Fisher*'s [1953] statistics. In general, samples preserve only one magnetization component, as seen in the *Zijderveld* [1967] diagrams (Figure 3), although a viscous component was removed at the first steps of AF demagnetization in some samples.

[11] The mean AF and thermal characteristic directions (Figure 4) are indistinguishable at a 99% confidence level (F = 1.44, Watson test as described by *Tauxe* [2002]). Therefore, all populations of magnetic minerals (lower and higher coercivities or unblocking temperatures) in the samples show the same remanence component indicating coeval magnetization. In view of these results, another set of 106 samples were cleaned using only AF. Ultimately, three or more specimens from each site were demagnetized.

[12] Samples from dropstones also retained significant magnetization (~40%) after being submitted to peak fields up to 160 mT, but the highest unblocking temperatures were only ~500°C (Figures 5a–5c). Samples from the basement (Bambuí Group) showed similar magnetic behavior during demagnetization as those from the Santa Fé Group. AF cleaning up to 160 mT eliminated less than 30% of the remanence, with temperatures up to 680°C required to completely erase magnetization (Figures 5d–5f). The only identified secondary component is similar to the present-day field.

[13] The mean ChRM for each site (stratigraphic level) was calculated on the basis of three or four specimen results (Table 1), and are displayed in Figure 6. The Santa Fé ChRMs are all of reversed polarity, compatible with the magnetization being acquired during the Permo-Carboniferous Reversed Superchron (PCRS). This direction is distinct from the characteristic directions of the BAM dropstones (see Table 2 and Figure 6a), and from the ChRMs of the Bambuí basement rocks (see Table 2 and Figure 6c), discarding the possibility of any intense event of remagnetization. Site mean distributions for BAM sections (Figure 6a) differ greatly probably because section A spans only 0.6 m while the 6 scattered sites of section B were taken from a much thicker (8 m) section. Site mean distribution of sections C and D (Lavado member; see Figure 6b) are indistinguishable although the sections are located ~100 km apart, suggesting they may cover the same time interval.

4. Magnetic Mineralogy and Anisotropy of Magnetic Susceptibility

[14] Variations in the remanence intensity (M/M_0) during the demagnetization procedures (Figure 2) indicates the presence of hematite (high coercivity and unblocking temperatures close to 680°C) and possibly magnetite (lower coercivities and unblocking temperature in the range 550–610°C). Isothermal remanent magnetization curves (IRM), acquired in a Pulse Magnetizer MMPM10, showed positive gradients for fields as high as 2.8 T indicating that samples did not reach saturation (Figure 7). Following *Kruiver et al.* [2001] the best adjustments were obtained using two magnetic components: one with a $B_{1/2} \cong 400$ mT (half the IRM saturation field) and other of about 60 mT (95% and 5% of the sample remanence, respectively). Hysteresis loops were obtained in a Molspin VSM magnetometer. The majority of samples (Figure 8) displayed a wasp-waist shape due to the mix of different coercivities [*McCabe and Channell*, 1994], which are in the range 55 to 237 mT. Saturation of magnetization occurred in the interval 0.6 to 1.7 μAm^2.

[15] Thermomagnetic experiments were performed in argon atmosphere using a KLY4CS−Kappabridge furnace. The curves (Figure 9) display features compatible with the presence of magnetite and hematite. Samples from both Lavado and Brejo do Arroz members have similar characteristics; heating curves show inflections near 530°C and 620°C, which are reproduced during cooling although susceptibility tend to be enhanced. All magnetic properties investigated here confirm the presence of magnetite in addition to hematite, corroborating *Campos and Dardenne*'s [1994] optical observations that magnetite is present in LM. Both minerals carry the same ChRM component, and therefore hematite might have acquired magnetization in the early stages of diagenesis.

[16] The anisotropy of magnetic susceptibility (AMS) of all samples was measured in a Kappabridge equipment before submitting specimens to magnetic cleaning routines. The majority of sites did not show any defined fabric due in part to the small number of analyzed specimens per site (3 to 4); those with consistency of the principal axes belong
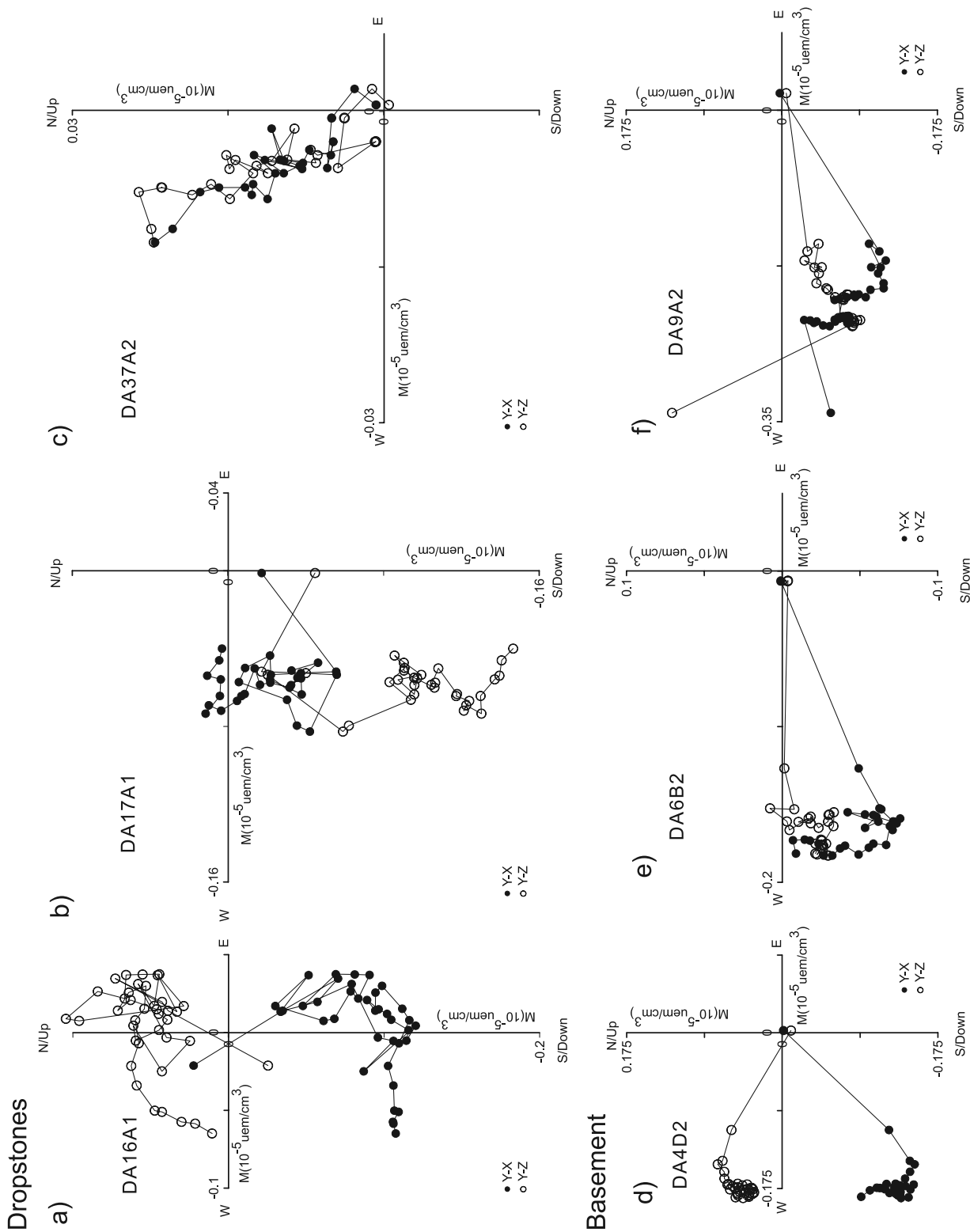
Figure 5. Orthogonal plots of the magnetic remanence during gradual demagnetization for (a–c) dropstone and (d–f) basement specimens. Open (solid) symbols are vertical (horizontal) projections.

Table 1. Paleomagnetic Results for the Santa Fé Group[a]

			Mean Characteristic Directions				Virtual Geomagnetic Poles			
	Site	Relative Position (m)	n/N	Declination (deg)	Inclination (deg)	α_{95} (deg)	k	PLong (deg E)	PLat (deg S)	dp (deg)	dm (deg)
Brejo do Arroz: Section A	11	0.00	3	170.1	38.9	13.9	80	16.4	79.6	9.9	16.6
	12	0.23	3	161.8	36.8	15.7	63	31.0	72.5	10.7	18.4
	13	0.28	3	172.6	42.3	10.3	145	357.2	80.1	7.8	12.7
	14	0.48	3	175.3	44.9	11.5	116	339.0	79.9	9.2	14.5
	15	0.53	3	174.9	38.7	11.8	111	0.6	83.5	8.3	14.0
Brejo do Arroz: Section B	38[b]	0.00	3	203.1	24.8	23.6	28	218.3	67.4	13.6	25.3
	18	5.00	4	152.7	51.0	10.0	85	8.3	61.1	9.1	13.5
	23[c]	5.40	3	117.6	43.7	11.5	116	24.4	31.6	9.0	14.4
	27[b]	5.50	4	158.3	53.9	21.5	19	358.0	63.7	21.1	30.1
	31[c]	5.90	3	88.7	55.2	13.2	87	9.7	8.6	13.4	18.8
	34[c]	8.40	3	101.4	55.4	8.4	214	11.4	18.8	8.5	12.0
Lavado: Section C1	64	0.00	3	153.8	69.4	9.6	166	338.1	48.3	14.0	16.4
	65[c]	0.30	3	81.4	75.4	12.7	96	342.3	10.9	21.3	23.3
	66	0.50	3	141.1	61.8	13.7	82	357.8	47.9	16.4	21.2
	67	0.70	3	177.6	61.2	9.6	167	318.7	64.4	11.3	14.7
	68	0.85	3	177.8	62.6	12.9	92	318.0	62.7	15.8	20.2
	69	0.95	3	141.7	58.0	13.4	86	3.5	50.1	14.5	19.7
	70	1.05	3	160.7	59.0	10.1	150	346.8	61.5	11.2	15.1
	71	1.20	4	164.1	75.4	14.1	43	324.5	42.9	23.7	25.8
	72	1.35	3	181.4	53.7	12.5	98	310.7	72.5	12.2	17.5
	73[b]	1.55	3	186.3	47.4	21.6	33	289.5	76.9	18.2	28.0
	74	1.95	3	213	67.2	15.1	38	283.3	47.5	20.8	25.1
	75	2.55	3	186.5	52.2	9.7	163	295.7	72.9	9.1	13.3
	76	2.75	3	187.9	56.7	14.8	71	297.3	68.3	15.5	21.4
	77	3.75	3	157.2	69.1	17.3	52	336	49.9	25.0	29.4
	78	4.75	4	167.2	56.7	7.4	153	340.9	66.6	7.8	10.7
	79	4.75	3	153.9	46.8	14.9	69	14.8	63.4	12.4	19.2
	80	5.00	3	133.1	58.8	11.1	124	5.4	43.5	12.3	16.5
	81	5.25	3	188.8	67.1	7.7	256	304.3	56.2	10.6	12.8
	82	5.52	3	152.0	58	14.9	69	357.1	57.2	16.2	22.0
	83	5.72	4	218.1	65.4	5.2	554	277.6	46.2	6.8	8.4
	84	6.12	3	189.8	57.4	14.7	71	294.4	67.1	15.7	21.5
	85	6.52	4	190.4	75.4	11.7	63	307.9	43.7	19.7	21.4
	86	6.82	4	199.6	75.1	13.8	46	302.2	42.7	23.0	25.2
Lavado: Section C2	56	1.95	3	166.4	63.6	15	68	333.5	59.3	18.8	23.8
	57	2.95	3	198.0	74.7	12.8	53	302.7	43.6	21.2	23.3
	58[b]	3.15	4	162.7	43.7	22.9	17	13.0	71.7	17.8	28.6
	59[b]	3.45	4	152.9	59.5	22.0	18	353.9	56.8	24.8	33.0
	60	3.65	3	170.5	47.7	10.0	154	348.9	75.1	8.5	13.0
	61	3.90	3	188.8	48.6	12.5	99	283.9	74.9	10.8	16.4
	62	3.90	3	186.3	57.1	13.5	84	301.0	68.3	14.3	19.7
	63	4.10	4	176.6	64.7	8.0	132	319.2	60.0	10.3	12.9
	40	6.82	3	191.3	64.4	12.2	104	299.3	59.1	15.6	19.5
	41	6.97	3	191.4	61.7	7.0	310	296.5	62.1	8.4	10.8
	42	7.07	3	191.0	54.2	11.1	124	288.0	69.5	11.0	15.6
	43	7.22	3	172.2	59.2	11.5	117	329.2	65.8	12.9	17.2
	44	7.37	3	176.7	64.8	8.7	199	319.1	59.9	11.3	14.0
	45	7.47	3	173.6	58.9	4.6	705	326.9	66.4	5.1	6.9
	46	7.67	3	163.5	62.2	8.8	196	338.8	59.8	10.7	13.7
	47	7.82	3	167.4	45.1	13.0	91	2.1	74.7	10.4	16.5
	48	8.02	3	147.1	49.4	12.4	100	14.3	57.1	10.9	16.5
	49	8.12	3	157.5	44.2	7.7	258	17.0	67.2	6.1	9.7
	50	8.12	4	184.6	52.8	14.7	40	301.4	72.9	14.0	20.3
	51	8.32	3	161.4	55.3	14.8	70	351.9	64.8	15.0	21.1
	52	8.37	4	192.0	56.9	7.7	255	289.9	66.7	8.1	11.2
	53	8.57	4	186.0	68.1	16.9	30	308.0	55.2	23.8	28.4
	54[c]	9.37	4	187.5	86.8	17.3	29	313.7	23.1	34.3	34.4
	55	9.62	3	201.8	50.6	11.6	114	264.9	65.4	10.5	15.6
Lavado: Section D	104	0.00	3	146.5	67.0	14.3	76	346.5	48.0	19.6	23.7
	103[b]	0.25	4	200.3	55.2	22.1	18	273.7	64.3	22.4	31.4
	102[b]	0.55	4	184.4	71.7	18.7	25	310.4	50.8	28.9	32.9
	101	1.05	4	150.8	64.9	17.4	29	347.0	52.0	22.6	28.0
	100	2.55	4	150.0	62.4	15.5	36	351.7	53.5	18.9	24.2
	99[b]	2.85	3	176.3	53.0	21.3	35	325.2	73.5	20.4	29.5
	98	2.85	4	167.4	48.6	15.0	38	355.5	73.3	13.0	19.7
	97	3.45	3	173.6	52.5	15.6	63	333.2	73.3	14.8	21.5
	96	3.85	3	170.7	45.5	8.0	238	354.6	77.2	6.5	10.2
	95	6.35	3	127.6	46.9	14.7	71	21.8	40.9	12.2	19.0
	94[b]	6.60	4	189.5	47.4	25.3	14	277.8	75.9	21.3	32.8
	93	6.80	3	180.8	35.5	16.7	55	295.4	87.7	11.2	19.3

Table 1. (continued)

	Site	Relative Position (m)	n/N	Mean Characteristic Directions				Virtual Geomagnetic Poles			
				Declination (deg)	Inclination (deg)	α_{95} (deg)	k	PLong (deg E)	PLat (deg S)	dp (deg)	dm (deg)
	92	7.00	3	166.0	61.4	9.3	175	336.7	62.2	11.0	14.3
	91	8.20	3	159.2	47.8	8.1	231	9.5	67.8	6.9	10.6
	90[b]	8.50	4	158.6	67.9	28.1	12	336.4	52.4	39.4	47.1
	89	8.75	3	143.6	64.9	10.0	154	351.6	48.0	13.0	16.1
	88[b]	10.05	3	177.1	50.1	19.9	39	324.8	76.3	17.8	26.6
	87	10.35	3	184.1	40.7	11.2	122	281.6	83.0	8.2	13.6
Brejo do Arroz mean			7	161.7	43.9	11.8	27	14.6	70.7	$\alpha_{95} = 14$	k = 18
Lavado mean			54	171.5	59.7	3.2	36	328.8	64.1	$\alpha_{95} = 4.3$	k = 21
Overall mean			60	171.0	58.0	3.2	34	330.9	65.7	$\alpha_{95} = 4.1$	k = 21

[a]Abbreviations are as follows: N, number of specimens for mean calculations; dp and dm, confidence oval of 95%; and α_{95} and k, *Fisher*'s [1953] statistical parameters.
[b]Rejected site $\alpha_{95} > 18°$.
[c]Rejected site $\Delta > 40°$.

mainly to section C of Lavado member which have bulk susceptibilities in the range $5-8.10^{-5}$ SI slightly higher than those in section D and BAM $(1-3.10^{-5}$ SI) as seen in Figure 10a. The ellipsoids evaluated by *Lienert*'s [1991] statistics show low degree of anisotropy (P = K1/K3) rarely exceeding 1.05 (Figure 10b) a behavior that normally coincides with higher susceptibilities. The few results for the BAM sections show the main axes K1 and K2 in the horizontal plane (oblate ellipsoids; see Figures 10c and 10d) in accordance with a low-energy sedimentary environment, probably a sizable water body. The LM sites show indistinctly oblate and prolate ellipsoids (Figure 10c), and a tendency for lineations in two directions (W-NW and N-NE) are seen in sections C and D. However, inclinations vary greatly, and probably reflect the lack of precision in the distinction of K1 and K2 axes as samples are practically isotropic. Despite that, the data is very helpful showing that the magnetic anisotropy had no clear influence on the remanent magnetization.

5. Discussion

[17] Magnetic declination and inclination variation through the investigated sections are displayed in Figure 11. The two

sections (C and D) show the same magnetic behavior although situated about 100 km apart. However, declinations in section C reach values greater than 180° more commonly than in section D, suggesting that they recorded different phases of the secular variation cycles. Therefore, combining the two sections is more likely to average out the geomagnetic secular variation. Paleomagnetic poles for the BAM and LM were calculated giving unit weight to the virtual geomagnetic poles (VGPs) of each site (Table 1). VGPs based on mean directions with high internal dispersion ($\alpha_{95} > 18°$), and those falling at an angular distance (Δ) greater than 40° from the mean were discarded, and are indicated in Table 1. After applying these criteria 54 sites from LM passed the selection, and the mean pole is located at 328.8°E 64.1°S ($\alpha_{95} = 4.3°$; k = 21). However, only 7 sites were selected for the BAM pole (14.6°E 70.7°S; $\alpha_{95} = 14.4$; k = 18), most of them from the shorter section A. The BAM sites alone are not sufficient to determine a reliable paleomagnetic pole; the small number of sites from a short section probably is not enough to average out secular variation. Considering that the two member may be locally interfingered (Figure 1; the relative stratigraphic position of the BAM and LM investigated sections are not known) there is no clear justification to separate results. In fact the BAM
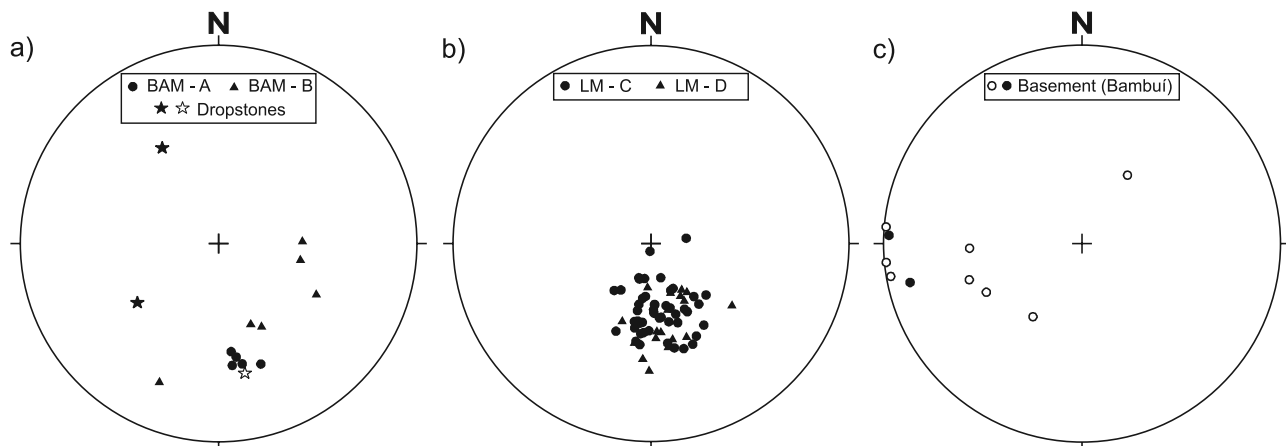

Figure 6. Stereo plots of site mean directions. (a) Brejo do Arroz member; sections A and B and dropstones. (b) Lavado member; sections C and D. (c) Bambuí Group (basement). Open (solid) symbols are negative (positive) inclinations.

Table 2. Characteristic Magnetic Directions for the Basement and Dropstones[a]

Site	Declination (deg)	Inclination (deg)	α_{95}[b] (deg)	n (N)	K
		Basement			
1	213.8	−42.6	26.7	3	22
2	243.4	−33.4	25.3	3	25
3	267.9	−31.0	42.0	2	37
4	252.5	−28.6	40.9	2	39
5	275.1	−0.5	28.8	2	77
6	272.6	1.5	18.7	3	45
7	257.4	6.9	17.8	2	198
8	264.7	−0.5	34.0	2	56
9	260.4	−1.4	15.8	2	252
10	33.4	−44.5	25.3	2	100
		Pebbles			
16	168.7	−34.2	(14.4)[b]	(19)	
17	234.4	36.9	(13.9)[b]	(9)	
37	329.5	−43.4	19.7	2	163

　[a]Abbreviations are as follows: α_{95} and k, *Fisher's* [1953] statistical parameters; n, number of specimens considered in the means; and N, number of steps.

　[b]Maximum angular deviation for N steps.

virtual poles are well inserted within the area delineated by those from LM (see the left-hand side of Figure 12). The distribution of the selected VGPs ($\alpha_{95} \leq 18°$ and $\Delta \leq 40°$) is slightly elongated as indicated by the elliptical area in the right-hand side of Figure 12, and is non-Fisherian at a 95% confidence level as indicated by the parameters M_U = 1.0028 (<1.207) and M_E = 1.1050 (>1.094) for a modified test of Kolgomorov-Smirnov [*Stephens*, 1974]. Conversely, the distribution of the corresponding magnetization directions (M_U = 0.9896; M_E = 0.8515) is Fisherian at the same confidence level.

[18] The resulting paleomagnetic pole for the Santa Fé Group (SF pole) is situated at 330.9°E 65.7°S (N = 60; α_{95} = 4.1°; k = 21), and satisfies most of the quality criteria required for a reference pole: large number of samples taken from various sections some of which ~100 km apart; thorough demagnetization of samples by both a.f. and thermal techniques; strong evidence for primary origin of magnetization on the basis of investigations of magnetic mineralogy; and presence of both magnetite and hematite carrying the same ChRM components which are distinct from the ones carried by samples from the basement and dropstones. The consistency of results from different sections guarantees the stability of the magnetization, and discards the possibility of any nonidentified tilting in the massive sedimentary rocks. The reversal test was not applicable as all sites display reversed magnetization which in turn corroborates the hypothesis of magnetization acquired during or shortly after deposition. Therefore the age of the SF pole is well constrained within the Permo-Carboniferous Reversed Superchron (PCRS or Kiaman; ~320–265) [*Opdyke et al.*, 2000].

[19] The SF along with other late Paleozoic poles for South America (SA) is plotted on Figure 13. For this plot all existing poles were considered except those determined solely from natural remanent magnetization or those clearly affected by rotations or secondary magnetizations. The database is displayed on Table 3. Several of the listed poles are based on few sites probably not enough to eliminate

secular variation effects, as discussed by *Van der Voo* [1990]. Nevertheless, they are included in this analysis as some of the poles on the basis of studies of igneous rocks fall into this low sample number category. These results need to be considered regardless of low sample number, since they supply absolute age data, and their thermoremanence may give a more reliable record of the primary magnetization than sediments do. Besides that, the existing database does not allow a particularly rigorous selection criterion. In Figure 13 the available poles are plotted according to the following age classification: middle-late Carboniferous, late Carboniferous-middle Permian, and middle Permian-early Triassic. Poles based on mixed polarity records, and on data from igneous rocks were indicated in the figure, as well as those based on syntectonic or post-tectonic magnetization.

[20] Poles are dispersed, allowing for some variation in the interpreted APWPs from late Carboniferous (lC) to early Triassic (eTr). One such proposed path [*Tomezzoli*, 2001, *Tomezzoli et al.*, 2006; *Rapalini et al.*, 2006] runs eastward (indicated by the hatched area), even though some of the component paleomagnetic poles may not be based on primary magnetization (20 to 26; see Table 3). The Tunas I pole (22; see *Tomezzoli and Vilas* [1999]) has a synfolding magnetization evidenced by stepwise tectonic tilt correction; the younger Tunas II pole (21; see *Tomezzoli* [2001]) leaves uncertain the synfolding or prefolding origin of magnetization. The Rio Curacó (20) and San Roberto (23) poles are from the upper and lower parts of the Carapacha Basin, respectively, and gave a negative fold test [*Tomezzoli et al.*, 2006]. The Cerro Colorado-Caminiaga (24), the Chancani (25) and the Rincón Blanco (26) poles were interpreted by the authors [*Geuna and Escosteguy*, 2004] to be remagnetized or tectonically affected as they plot near the geographic pole.

[21] A different path running westward may be envisaged considering the other poles in the late Carboniferous-middle Permian interval. An important consideration in this exercise regards the recorded polarities, given that the considered time interval includes the PCRS. A group of poles (16, 17 and 18; see Table 3) including normal and reversed polarities, and ages within 309–290 Ma interval are possibly correlated to the 305-Ma short normal polarity event found in the base of the PCRS [*Alva-Valdivia et al.*, 2002].

[22] The other set of late Carboniferous-middle Permian poles, all of reversed polarity, must be distinguished from the previous one, and may represent a younger age group within the PCRS. To this group belongs the SF pole besides the two poles (11 and 12) from the Itararé Group (Paraná Basin, southern Brazil). The Rio do Sul pole [*Franco*, 2007] is based on data from 9 m of shaly rhythmites, and plots near the older Itararé pole [*Pascholati*, 1983]. The relative stratigraphic position of these two poles is unclear as the original Itararé pole (11) includes data from different areas of the basin; a younger age for Rio do Sul pole cannot be ruled out, however pole 11 is of questionable reliability as is based on poorly constrained characteristic magnetization (not based on stepwise demagnetization). These observations are also valid for the red beds of the Los Colorados pole (13; see *Embleton* [1970]) which plot very close to 11. The other poles of the group are from the La Tabla igneous
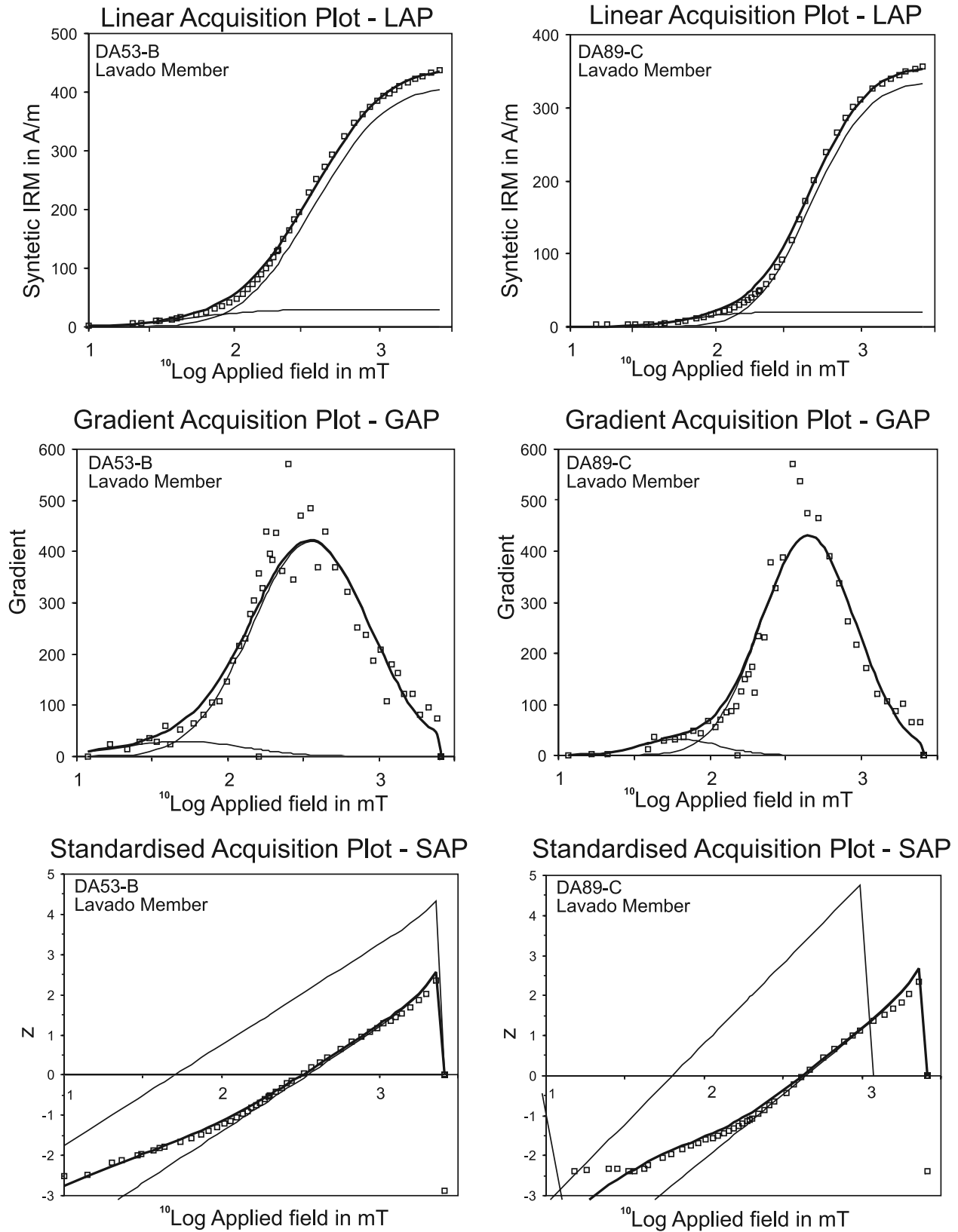
Figure 7. Examples of IRM curves and the analysis of *Kruiver et al.* [2001] for samples from Lavado member. Bold line is the total curve (sum of the two components with different coercivities).
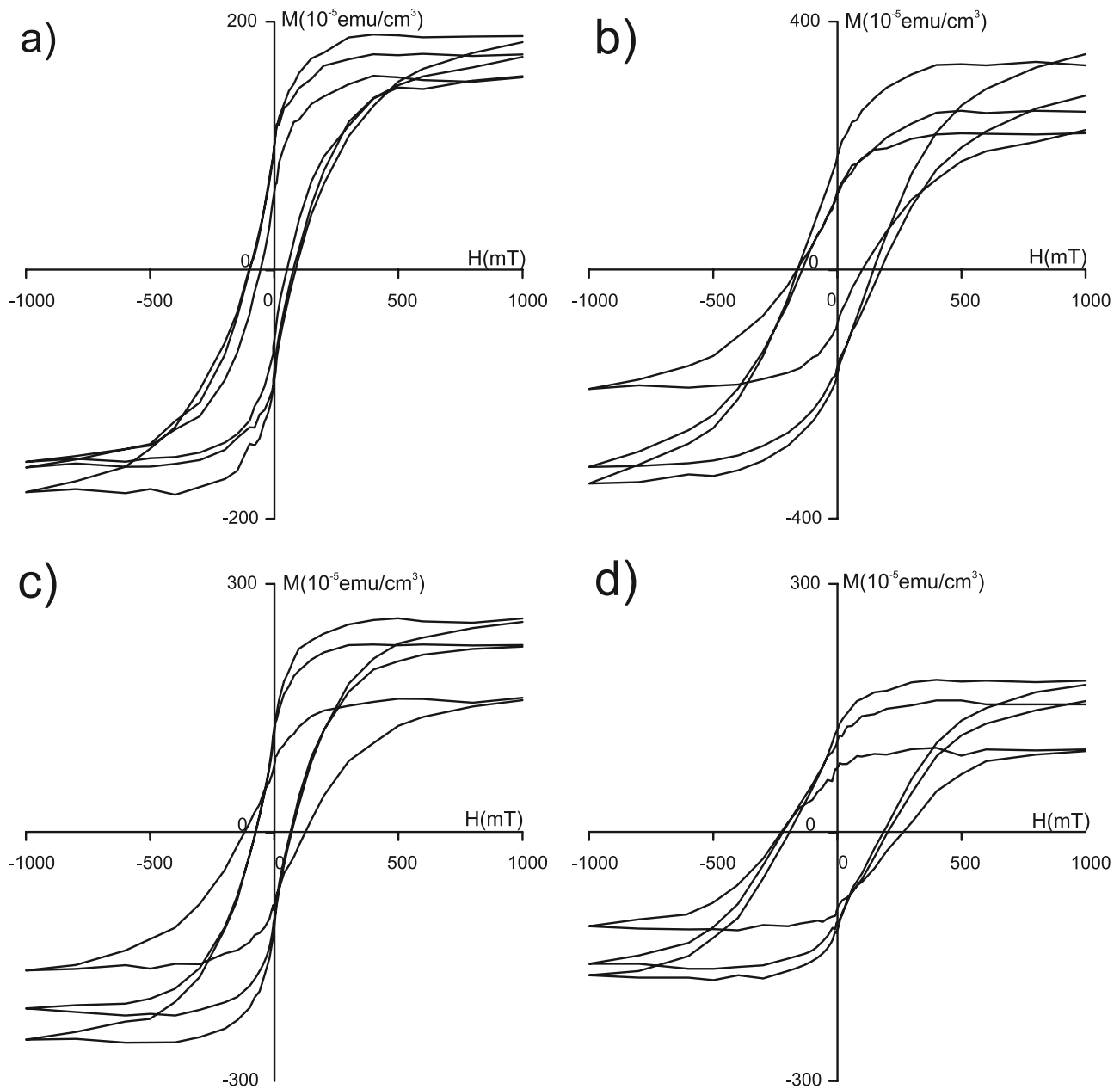
Figure 8. Examples of hysteresis loops for: Brejo do Arroz member (a) section A and (b) section B, as well as Lavado member (c) section C and (d) section D.
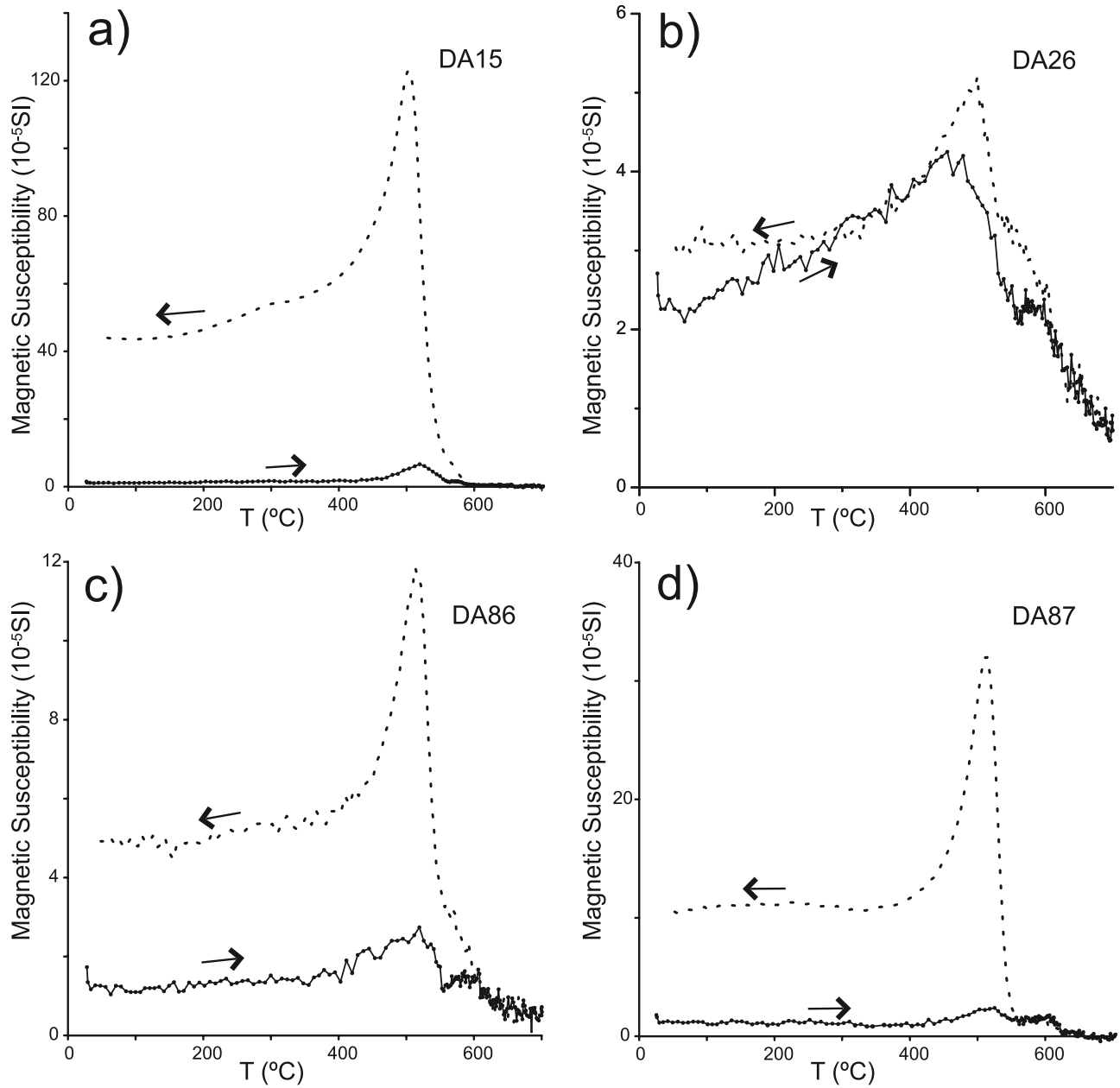
Figure 9. Examples of thermomagnetic curves for Brejo do Arroz member (a) section A and (b) section B, as well as Lavado member (c) section C and (d) section D. Solid and dashed lines are heating and cooling curves, respectively.
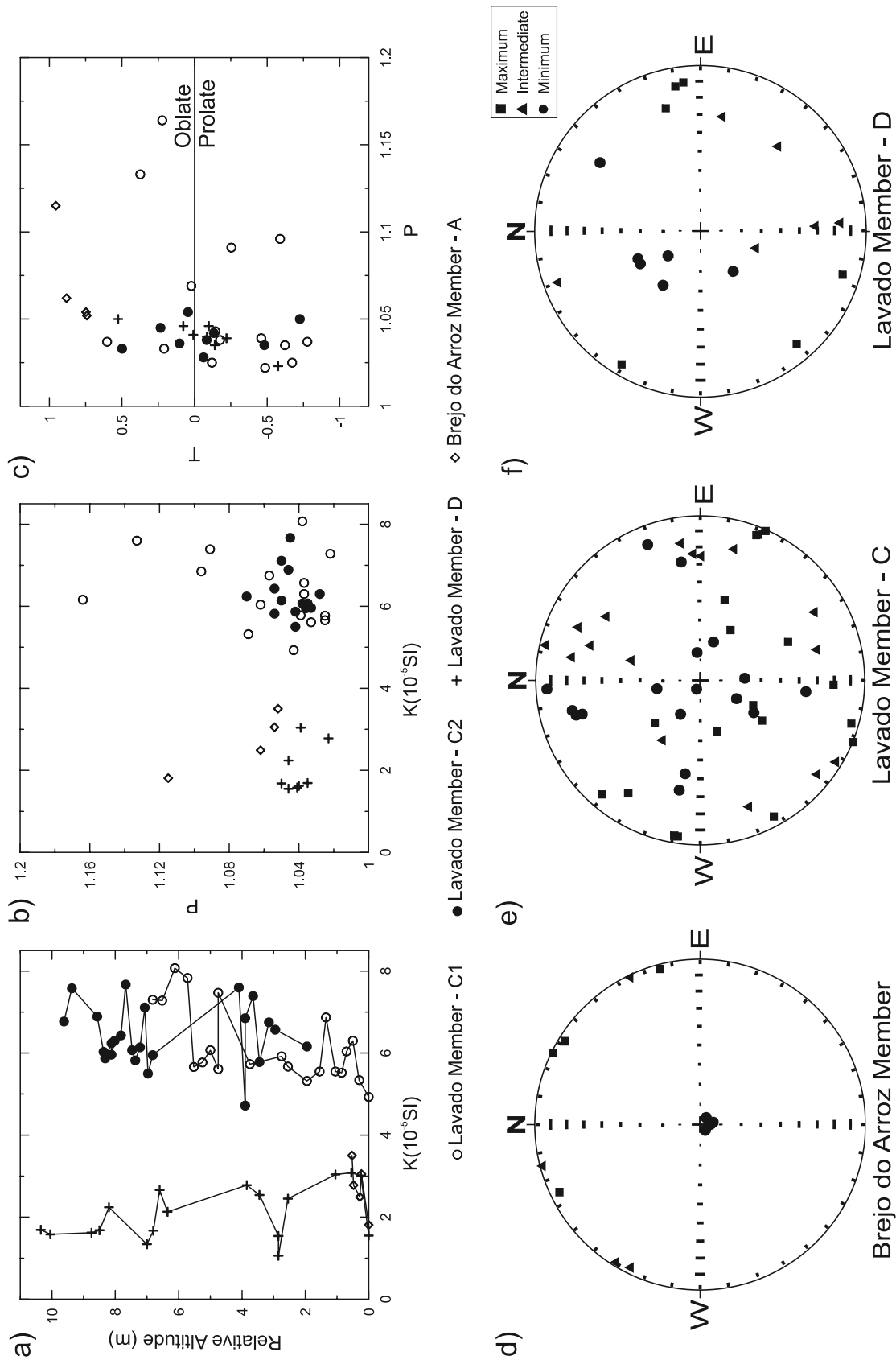
Figure 10. (a) Magnetic susceptibility throughout the studied sections. (b) Plot of the anisotropy degree (P = K1/K3) versus bulk susceptibility (K). (c) Plot of the shape parameter (T = 2*ln(K2/K3)/ln(K1/K3) −1) versus P. Mean principal axes: (d) Brejo do Arroz member section A and Lavado member (e) section C and (f) section D.
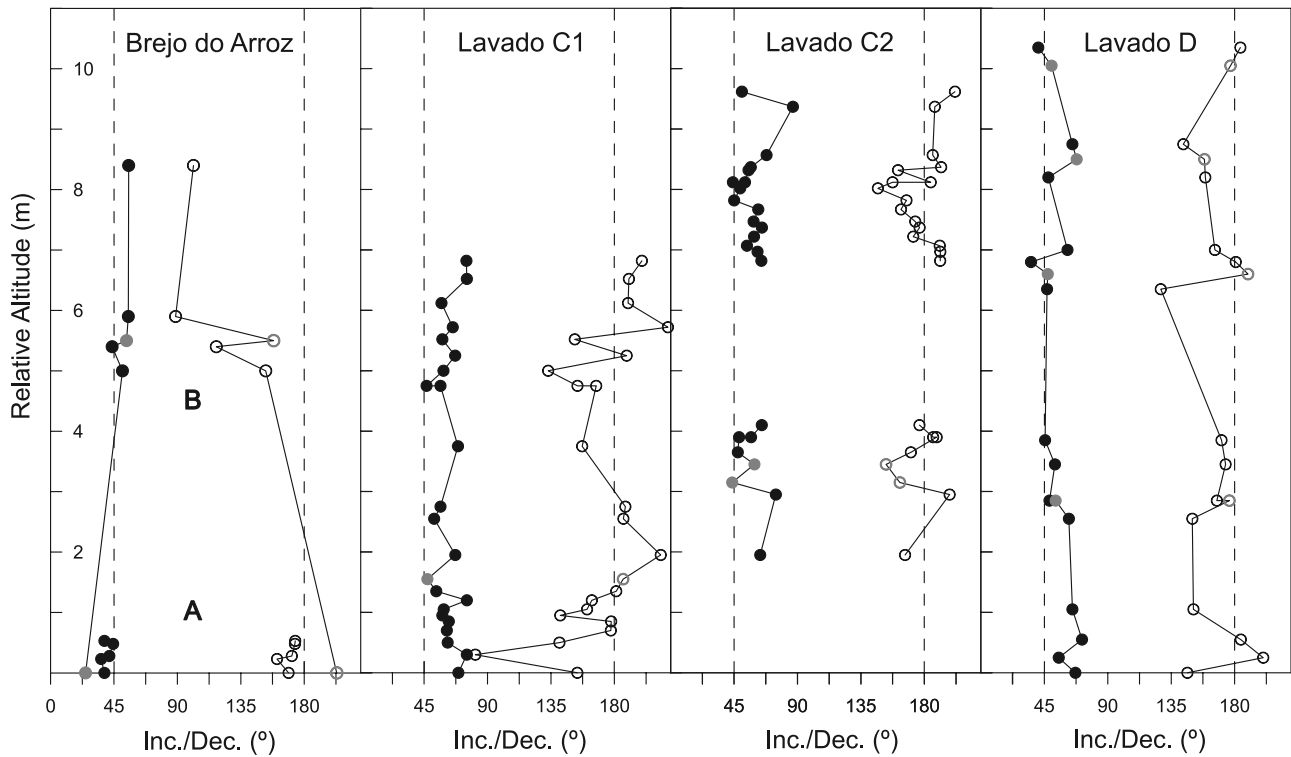
Figure 11. Variation of declination (Dec.) and inclination (Inc.) throughout stratigraphy for all investigated sections. Open and solid symbols are declinations and inclinations, respectively. Grey symbols indicate poorly defined mean directions ($\alpha_{95} > 18°$).

rocks (15; see *Jesinkey et al.*, 1987]) from Chile, and the Copacabana limestones from Peru (10; see *Rakotosolofo et al.* [2006]) which remanence is carried by magnetites. Poles 20 and 22 (Curacó and Tunas I, respectively) plot near the reversed late Carboniferous-middle Permian pole group,

however due to the evidences for a nonprimary origin of the magnetization they will not be included.

[23] The majority of the poles in the middle Permian-early Triassic group has mixed polarities excepting the Irati (1), of normal polarity, and the Ceará-Mirim (7) and the
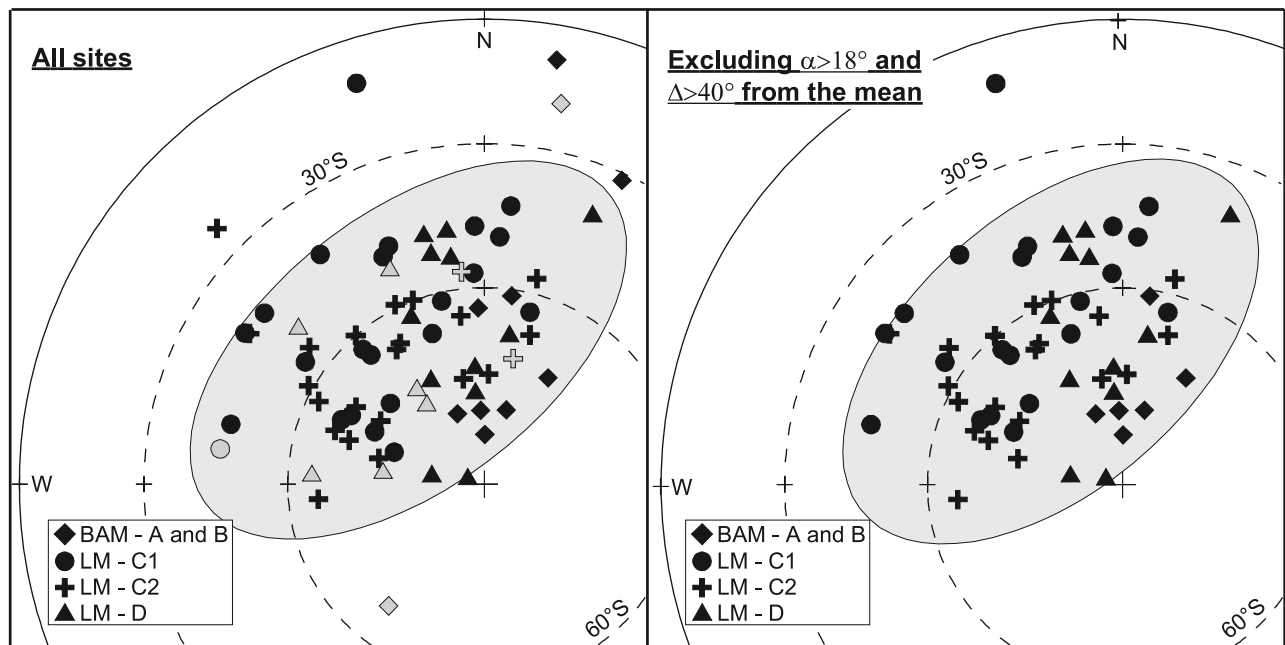
Figure 12. Distribution of the VGPs of the Santa Fé sites in a Schmidt projection. Shadowed area indicates where most of data concentrate before and after excluding sites with $\alpha_{95} > 18°$ (light color symbols), and angular distance from the mean $\Delta > 40°$.
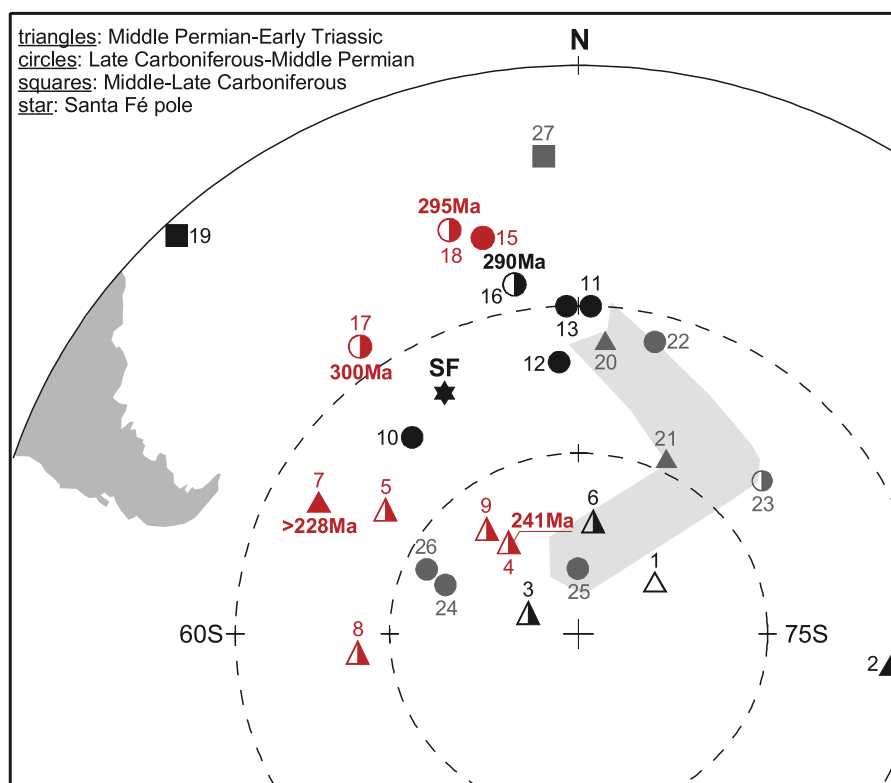
Figure 13. Plot of the late Paleozoic paleomagnetic poles from South America. Symbols are as follows: red, igneous rocks; grey, syntectonic or posttectonic magnetization; half solid, mixed polarities; squares, middle to late Carboniferous; circles, late Carboniferous–middle Permian; triangles, middle Permian–early Triassic. Radiometric ages are indicated when available. Numbers correspond to pole numbers listed in Table 3.

Amaná (2) of reversed polarity. The first one has poorly constrained magnetization, and the pole position resembles those of the early Cretaceous from the igneous rocks of the Serra Geral Formation [*Ernesto et al.*, 1999]. The age of the Ceará-Mirim pole [*Ernesto et al.*, 2003] indicated in Figure 13 corresponds to the oldest reported age for the dyke swarm, although numerous Ar/Ar dating points to an early Cretaceous age. Considering the uncertainty in age and the discordant polarity, this pole might not be included in the middle Permian-early Triassic group. The Amaná pole is completely discordant from other poles of the group.

[24] On the basis of the aforementioned pole groups an APWP for South America is proposed for middle Carboniferous to early Triassic. The middle Carboniferous (mC) is represented only by the Tepuel pole (19; see *Rapalini et al.* [1994]) as the Hoyada Verde (27; see *Rapalini and Vilas* [1991]) rocks carry a syntectonic magnetization; a late Carboniferous (lC) mean pole may be calculated based on the mixed polarity poles (16 to 18) with age probably around 305 Ma; the reversed polarity group (10 to 15) probably encompass a wide range of ages probably centered at an early Permian (eP) age. The mean of this group is not considerably changed (Table 4) if pole 22 (Tunas I) is included. The middle Permian to early Triassic group discussed above will give a mean pole to which we will attribute a Permo-Triassic (P-Tr) age, as the only age reference for this group is given by the Ar/Ar dating of

~241 Ma for the Alto Paraguay Province [*Velázquez et al.*, 1996].

[25] For calculating the mean poles (Table 4) data were corrected for intraplate rotations [*Schettino and Scotese*, 2005]. The applied corrections are small, and do not result in any significant modification to the mean poles as displayed in Figure 14. A proposed APWP based on these mean poles (Figure 14) may represent an oversimplification of the South America drifting path. The large confidence α_{95} statistic parameter of the mean poles may reflect the lack of rigorous selection of poles, and age mixing. The Santa Fé and Copacabana (10) poles positioning in relation to the new path clearly suggests that they should be separated from the here named early Permian group. However, considering the scarcity of data, poor quality of the majority of poles, and age uncertainties, this smooth curve is preferable for practical purposes, while more and better reference poles are not available.

6. Concluding Remarks

[26] The APWP segment from late Carboniferous to early Triassic proposed here encompasses a time interval of 64 Ma for a plate drift of about 29°, implying in a mean velocity of ~5.0 cm/a. When compared to the present displacements of 1−3 cm/a for the larger lithospheric blocks the calculated velocity is high considering the huge dimensions of the

Table 3. South American Late Paleozoic Paleomagnetic Poles[a]

Identification	Rock Type	Polarity	Age	PLong (deg E)	PLat (deg S)	NS	α_{95} (deg)	Pole Number	Reference
Stable Areas or Pretectonic Magnetization									
Irati Fm., Paraná Basin, Brazil	Sediments	N	P-Tr	54	83	6	3.4	1	Pascholati et al. [1976]
Amaná Fm., Paganzo Basin, NW Argentina	sediments	R	eTr	96	63	14	11.0	2	Sinito et al. [1979]
Corumbataí Fm., Paraná Basin, Brazil	sediments	N/R	P-Tr	294	86	15	14	3	Valencio et al. [1975]
Alto Paraguay Province, Brazil-Paraguay border	igneous	N/R	241.5 ± 1.3[b]	324	81	32	6.2	4	Ernesto [2005]
Mitu Group, Bagua Grande area, western Peru	sediments/igneous	N/R	P-Tr	304	71	6	5.7	5	Gilder et al. [2003]
Independencia Group, Paraná Basin, Paraguay	sediments	N/R	P-Tr	7	81	10	6.6	6	Rapalini et al. [2006]
Ceará Mirim II dykes, NE Brazil	igneous	R	>228[c]	298	65	18	6.5	7	Ernesto et al. [2003]
Horcajo, Andean Chain, Argentina	igneous	N/R	lP	265	72	26	12	8	Rapalini and Vilas [1991]
Tambillos, Andean Chain, Argentina	igneous	R	mP	320	79	16	6.5	9	Rapalini and Vilas [1991]
Copacabana Group, subandean zone, Peru	sediments	R	eP	321	68	9	5.2	10	Rakotosolofo et al. [2006]
Itararé, Paraná Basin, Brazil	sediments	R	P-C	2	60	44	3.9	11	Pascholati [1983]
Rio do Sul rhythmites, Paraná Basin, Brazil	sediments	R	P-C	356	66	58	2.2	12	Franco [2007]
Los Colorados, Paganzo Basin, Brazil	redbeds	R	P-C	358	60	26	3.5	13	Embleton [1970]
Santa Fé Gr., Sanfranciscana Basin, central Brazil	sediments	R	P-C	331	66	60	4.1	14	this paper
La Tabla Fm., Atacama Desert, Chile	igneous	R	P-C	347	51	10	5.7	15	Jesinkey et al. [1987]
Pular and Cas Fm., Atacama Desert, Chile	sediments	N/R	290 ± 7[c]	350	57	10	9.6	16	Jesinkey et al. [1987]
Lago Ranco granites, Central Valley, Chile	igneous	N/R	295 ± 7/309 ± 8[c]	324	57	7	18.8	17	Beck et al. [1991]
La Colina Fm., Argentina	redbeds/flow	N/R	295 ± 5[c]	343	49	57	5.0	18	Sinito et al. [1979]
Tepuel Fm., Central Patagonia, Argentina	sediments	R	mC	316	32	16	8.5	19	Rapalini et al. [1994]
Syntectonic or Posttectonic Magnetization									
Rio Curacó, upper Carapacha Basin, Argentina	sediments/igneous	R	lP	5	64	13	5	20	Tomezzoli et al. [2006]
Tunas Fm. II, Sierras Autrales, Argentina	sediments	R	eP-lP	26	74	24	5.2	21	Tomezzoli [2001]
Tunas Formation I, Sierras Autrales, Argentina	sediments	R	eP	14	63	19	5.4	22	Tomezzoli and Vilas [1999]
San Roberto Fm., lower Carapacha Basin, Argentina	sediments	N/R	eP	49	70	5	11	23	Tomezzoli et al. [2006]
Cerro Colorado-Caminiaga Fm., Paganzo Basin, Argentina	sediments	R	P-C	291	79	6	8.0	24	Geuna and Escosteguy [2004]
Chancani Fm., Paganzo Basin, Argentina	sediments	R	P-C	359	85	3	8.8	25	Geuna and Escosteguy [2004]
Rincon Blanco Volc. and Sed., Paganzo Basin, Argentina	sediments/volcanic	R	P-C	294	77	19	4.9	26	Geuna and Escosteguy [2004]
Hoyada Verde Fm., Andean Chain, Argentina	sediments	R	mC	356	42	18	8.3/6	27	Rapalini and Vilas [1991]

[a] Abbreviations are as follows: R, reversed polarity; N, normal polarity; N/R, mixed polarity; PLong, pole longitude; Plat, pole latitude; NS, number of considered sites in the mean; α95, semiangle of the cone of 95% confidence; and k, precision parameter [*Fisher*, 1953].

[b] Ar/Ar age.

[c] K-Ar age.

Table 4. Mean Late Paleozoic Poles for South America[a]

Age Interval	Pole Number	N	Longitude (deg E)	Latitude (deg S)	α_{95} (deg)
Middle Permian-early Triassic (mP-eTr)	3–6, 8, 9	6	311.0	80.0	6.9
Early Permian (eP); A	10–15	6	347.6	62.4	8.1
Early Permian (eP); B	10–15, 22	7	351.7	62.5	7.6
Late Carboniferous (lC)	16–18	3	341.0	54.3	12.4
Middle Carboniferous (mC)	18	1	317.5	31.6	-

[a]Abbreviations are the same as in Table 3.

Gondwana supercontinent, and even higher if Pangea is considered. Higher rates (~10 cm/a) are required if the longer eastward path are assumed, as the one proposed by *Tomezzoli et al.* [2006]. Owing to the great uncertainties in the South America mean paleomagnetic poles, the 345–270 Ma Laurentia APWP [*McElhinny and McFadden*, 2000] segment when rotated to South America to fit the classical Pangea A [*Lottes and Rowley*, 1990] is totally inserted within the large α_{95} cone of confidence of the lC South America pole (Figure 15). However, this confidence circle partially overlaps the 345–315 Ma segment of the Laurentia path in the alternative configuration (Pangea B; see *Morel and Irving* [1981]). The mean eP pole overlaps both curves, and the mP-eTr tends to fit the Pangea B reconstruction. It is important to keep in mind that the lC pole is based mainly on data from igneous rocks, and that the other two mean poles may represent large time intervals.
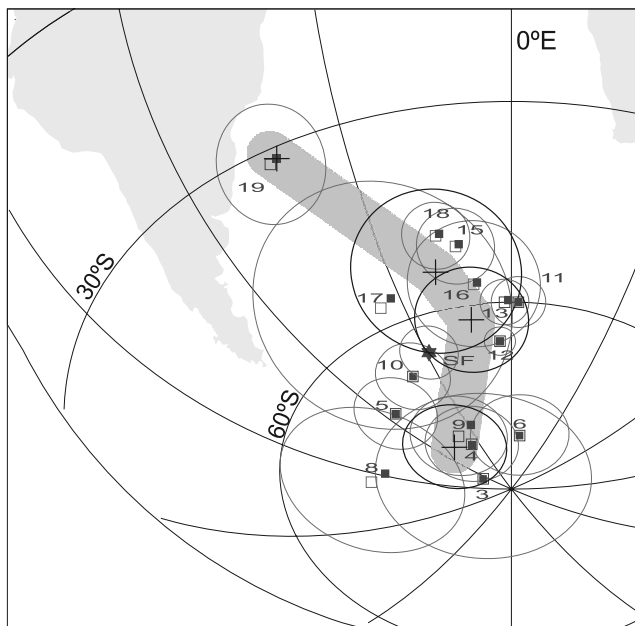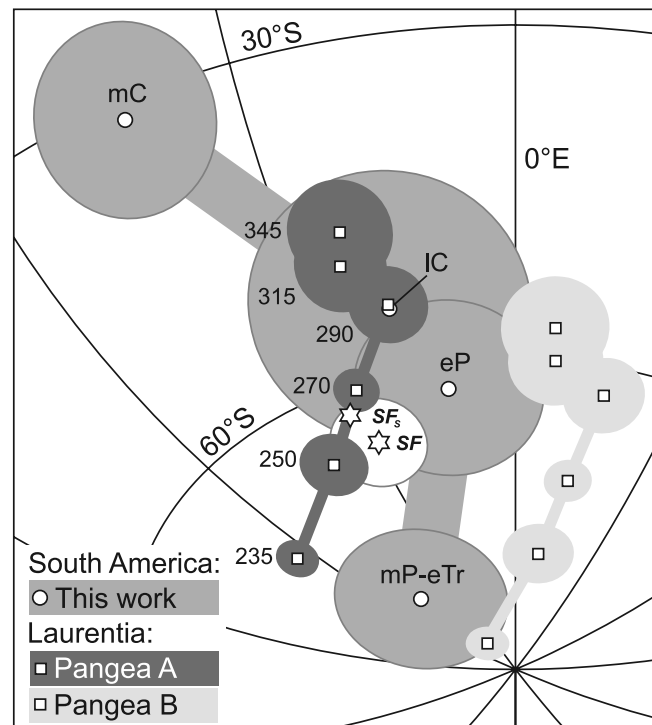
Figure 15. Plot of the South America path calculated in this work for the period middle Carboniferous to early Triassic (open circles) and the Laurentia path (open squares) [*McElhinny and McFadden*, 2000] rotated to South America in the Pangea A configuration (dark grey curve) [*Lottes and Rowley*, 1990] and Pangea B configuration (light grey curve) [*Irving*, 1977]. The Santa Fé pole before (SF) and after (SF$_S$) shallowing correction is also plotted.

[27] When we analyze the high-quality SF pole alone, it comes clear that it matches the Laurentia path in configuration A, and moves even closer if the shallowing correction envisaged by *Tauxe and Kent* [2004] is applied (Figure 15). This method is based on the distribution shape of magnetization directions predicted by a statistical field model. In order to evaluate the distribution shape a data set of at least 100 good-statistic sites must be available, a number greater than the existing SFG sites. This problem was overcome by using a set of 193 sample results corresponding to the good-statistic SF sites, which produced a distribution relate to a flattening factor f = 0.8. This means an inclination increase of only 3.6° (declination, 171.2°; inclination, 62.3°), and a corrected paleomagnetic pole at 328.3°E 62.5°S (Figure 15). This shallowing might be seen as a maximum value as the f factor changes for different cutoffs: $\Delta = 45°$ (197 samples) and $\Delta = 30°$ (187 samples) produce f = 1.0, that is to say, no shallowing. These results do not conflict with the observation that the sediments in the Sanfranciscana Basin underwent mild compaction [*Campos and Dardenne*, 1994], and indicates that sedimentation took place at much higher latitudes (39 to 44°) than its present location.

[28] The results presented above strongly suggest that the overlap of the continents found so far is an artifact of ill determined paleomagnetic poles, and that a Pangea A-type fit is possible if a larger and better data set become

Figure 14. Selected paleomagnetic poles (see section 5) and their confidence circles. The APWP fits the mean poles (crosses) in Table 5. For comparison, original (open squares) and rotated (solid squares) South American poles are plotted. Intraplate rotations are as proposed by *Schettino and Scotese* [2005].

available. *Van der Voo and Torsvik* [2004] came to similar conclusion with respect to Europe.

References

Alva-Valdivia, L. M., A. Goguitchaichvili, M. Grajales, A. F. de Dios, J. Urrutia-Fucugauchi, C. Rosales, and J. Morales (2002), Further constraints for Permo-Carboniferous magnetostratigraphy: Case study of the sedimentary sequence from San Salvador–Pantlanoaya (Mexico), *C. R. Geosci.*, *334*(11), 811–817, doi:10.1016/S1631-0713(02)01821-7.

Beck, M. E., A. R. Garcia, R. F. Burmester, F. H. Munizaga, F. A. Herve, and R. E. Drake (1991), Paleomagnetism and geochronology of late Paleozoic granitic rocks from the Lake District of southern Chile: Implications for accretionary tectonics, *Geology*, *19*(4), 332–335, doi:10.1130/0091-7613(1991)019<0332:PAGOLP>2.3.CO;2.

Briden, J. C., and M. W. McElhinny (2004), Evolution of the APWP for Gondwana: Constraints based on the geology of eastern Australia, *Eos Trans. AGU*, *85*(47), Fall Meet. Suppl., Abstract U32A-04.

Campos, J. E. G., and M. A. Dardenne (1994), The Neopaleozoic glaciation in the southern portion of Sanfranciscana Basin, *Rev. Bras. Geocienc.*, *24*, 65–76.

Campos, J. E. G., and M. A. Dardenne (1997a), Stratigraphy and sedimentation of the Sanfranciscana Basin: A review, *Rev. Bras. Geocienc.*, *27*, 269–282.

Campos, J. E. G., and M. A. Dardenne (1997b), Origin and tectonic evolution of the Sanfranciscana Basin, *Rev. Bras. Geocienc.*, *27*, 283–294.

Creer, K. M. (1970), A paleomagnetic survey of South American rock formations, *Philos. Trans. R. Soc. London, Ser. A*, *267*, 457–558.

Daemon, R. F., and L. P. Quadros (1970), Bioestratigrafia do Neopaleozóico da Bacia do Paraná, in *Proceedings XXIV Congresso Brasileiro de Geologia*, pp. 359–412, SBG, Brazil.

Embleton, B. J. J. (1970), Paleomagnetic results for the Permian of South America and a comparison with the African and Australian data, *Geophys. J.R. Astron. Soc.*, *21*(2), 105–118, doi:10.1111/j.1365-246X.1970.tb01770.x..

Ernesto, M. (2005), New early Triassic paleomagnetic pole for South America from the Alto Paraguay alkaline province, *Eos Trans. AGU*, *86*(18), Jt. Assem. Suppl., Abstract GP-41A–08.

Ernesto, M., M. I. B. Raposo, L. S. Marques, L. A. Diogo, and A. de Min (1999), Paleomagnetism and geochemistry of the magmatic rocks from northeastern Paraná magmatic province: Regional tectonic implications, *J. Geodyn.*, *28*, 321–340, doi:10.1016/S0264-3707(99)00013-7.

Ernesto, M., G. Bellieni, E. M. Piccirillo, L. S. Marques, A. de Min, I. G. Pacca, G. Martins, and J. W. P. Macedo (2003), Paleomagnetic and geochemical constraints on the timing and duration of the CAMP activity in northeastern Brazil, in *The Central Atlantic Magmatic Province*, *Geophys. Monogr. Ser.*, vol. 136, edited by W. E. Hames, J. G. McHone, and P. R. Renne, pp. 129–149, AGU, Washington, D.C.

Fisher, R. A. (1953), Dispersion on a sphere, *Proc. R. Soc. London, Ser. A*, *217*, 295–305, doi:10.1098/rspa.1953.0064.

Franco, D. R. (2007), Magnetoestratigrafia e análise espectral de ritmitos permocarboníferos da bacia do Paraná: Influências dos ciclos orbitais no regime deposicional, 176 pp., Univ. of São Paulo, São Paulo, Brazil.

Geuna, S. E., and L. D. Escosteguy (2004), Palaeomagnetism of the upper Carboniferous–lower Permian transition from Paganzo basin, Argentina, *Geophys. J. Int.*, *157*(3), 1071–1089, doi:10.1111/j.1365-246X.2004.02229.x.

Gilder, S., S. Rousse, D. Farber, B. McNulty, T. Sempere, V. Torres, and O. Palacios (2003), Post-middle Oligocene origin of paleomagnetic rotations in upper Permian to lower Jurassic rocks from northern and southern Peru, *Earth Planet. Sci. Lett.*, *210*(1–2), 233–248, doi:10.1016/S0012-821X (03)00102-X.

Guerra-Sommer, M., J. O. S. Santos, M. Cazzulo-Klepzig, L. A. Hartmann, R. Menegat, and N. J. McNaughton (2006), The geochronological significance of tonsteins in coal-bearing strata from the southern Paraná Basin, Brazil, paper presented at V South American Symposium on Isotope Geology, Univ. de la Repub., Punta del Este, Uruguay, 24–27 Apr.

Iannuzzi, R. (2008), Biostratigraphic versus geochronologic frameworks in the early Permian from Paraná Basin: Looking forward a possible consensus, in *I Symposium on Problems in Western Gondwana Geology I*, extended abstracts, pp. 72–78, RGEOTEC, Gramado, Brazil.

Irving, E. (1977), Drift of the major continental blocks since the Devonian, *Nature*, *270*, 304–309, doi:10.1038/270304a0.

Jesinkey, C., R. D. Forsythe, C. Mpodozis, and J. Davidson (1987), Concordant late Paleozoic paleomagnetizations from the Atacama Desert: Implications for tectonic models of the Chilean Andes, *Earth Planet. Sci. Lett.*, *85*(4), 461–472, doi:10.1016/0012-821X(87)90141-5.

Kirschvink, J. L. (1980), The least-squares line and plane and the analysis of paleomagnetic data, *Geophys. J.R. Astron. Soc.*, *62*(3), 699–718, doi:10.1111/j.1365-246X.1980.tb02601.x.

Kruiver, P. P., M. J. Dekkers, and D. Heslop (2001), Quantification of magnetic coercivity by the analysis of acquisition curves of isothermal remanent magnetization, *Earth Planet. Sci. Lett.*, *189*(3–4), 269–276, doi:10.1016/S0012-821X(01)00367-3.

Lienert, B. R. (1991), Monte Carlo simulation of errors in the anisotropy of magnetic susceptibility: A second-rank symmetric tensor, *J. Geophys. Res.*, *96*, 19,539–19,544, doi:10.1029/91JB02052.

Lottes, A. L., and D. B. Rowley (1990), Reconstruction of the Laurasian and Gondwandan segments of Permian Pangea, *Geol. Soc. Mem.*, *12*, 383–395, doi:10.1144/GSL.MEM.1990.012.01.36.

MacDonald, W. D. (1980), Net tectonic rotation, apparent tectonic rotation, and the structural tilt correction in paleomagnetic studies, *J. Geophys. Res.*, *85*, 3659–3669, doi:10.1029/JB085iB07p03659.

Matos, S. L. F., J. K. Yamamoto, C. Riccomini, J. Hachiro, and C. C. G. Tassinari (2001), Absolute dating of Permian ash-fall in the Rio Bonito Formation, Paraná Basin, Brazil, *Gondwana Res.*, *4*(3), 421–426, doi:10.1016/S1342-937X(05)70341-5.

McCabe, C., and J. E. T. Channell (1994), Late Paleozoic remagnetization in limestones of the Craven Basin (northern England) and the rock magnetic fingerprint of remagnetized sedimentary carbonates, *J. Geophys. Res.*, *99*, 4603–4612, doi:10.1029/93JB02802.

McElhinny, M. W., and P. L. McFadden (2000), *Paleomagnetism, Continents and Oceans*, *Int. Geophys. Ser.*, vol. 73, 386 pp., Elsevier, New York.

McElhinny, M. W., C. M. Powell, and S. A. Pisarevsky (2003), Paleozoic Terranes of eastern Australia and the drift history of Gondwana, *Tectonophysics*, *362*(1–4), 41–65, doi:10.1016/S0040-1951(02)00630-3.

Morel, P., and E. Irving (1981), Palaeomagnetism and the evolution of Pangea, *J. Geophys. Res.*, *86*, 1858–1872, doi:10.1029/JB086iB03p01858.

Muttoni, G., D. V. Kent, E. Garzanti, P. Brack, N. Abrahamsen, and M. Gaetani (2003), Early Permian Pangea 'B' to Late Permian Pangea 'A,' *Earth Planet. Sci. Lett.*, *215*(3–4), 379–394, doi:10.1016/S0012-821X(03)00452-7.

Opdyke, N. D., J. Roberts, J. Claoué-Long, E. Irving, and P. J. Jones (2000), Base of the Kiaman: Its definition and global stratigraphic significance, *Geol. Soc. Am. Bull.*, *112*(9), 1315–1341, doi:10.1130/0016-7606(2000)112<1315:BOTKID>2.0.CO;2.

Pascholati, E. M. (1983), Possibilidade de interferencias termais do magnetismo Juro-cretácico na análise paleomagnética do Grupo Itararé, in *Atlas do 4° Simposio Regional de Geologia*, pp. 211–222, SBG, São Paulo, Brazil.

Pascholati, E. M., I. G. Pacca, and J. F. Vilas (1976), Paleomagnetism of sedimentary rocks from the Permian Irati Formation, southern Brazil, *Rev. Bras. Geocienc.*, *6*, 156–163.

Pueyo, E. L., A. Pocovi, J. M. Parés, H. Millan, and J. C. Larasoaña (2003), Thrust ramp geometry and spurious rotations of paleomagnetic vectors, *Stud. Geophys. Geod.*, *47*(2), 331–357, doi:10.1023/A:1023775725268.

Rakotosolofo, N. A., J. A. Tait, V. Carlotto, and J. Cárdenas (2006), Paleomagnetic results from the early Permian Copacabana Group, southern Peru: Implication for Pangea palaeogeography, *Tectonophysics*, *413*(3–4), 287–299, doi:10.1016/j.tecto.2005.10.043.

Rapalini, A. E., and J. F. Vilas (1991), Tectonic rotations in the late Paleozoic continental margin of southern South America determined and dated by paleomagnetism, *Geophys. J. Int.*, *107*(2), 333–351, doi:10.1111/j.1365-246X.1991.tb00829.x.

Rapalini, A. E., D. H. Tarling, P. Turner, S. Flint, and J. F. Vilas (1994), Paleomagnetism of the Carboniferous Tepuel Group, central Patagonia, Argentina, *Tectonics*, *13*(5), 1277–1294, doi:10.1029/94TC00799.

Rapalini, A. E., S. Fazzito, and D. Orué (2006), A new late Permian paleomagnetic pole for stable South America: The Independencia Group, eastern Paraguay, *Earth Planets Space*, *58*(10), 1247–1253.

Rocha-Campos, A. C., M. A. S. Basei, A. Nutman, and P. R. dos Santos (2006), SHRIMP U-Pb zircon geochronological calibration of the late Paleozoic supersequence, Paraná Basin, Brazil, paper presented at V South American Symposium on Isotope Geology, Univ. de la Repub., Punta del Este, Uruguay, 24–27 Apr.

Schettino, A., and C. R. Scotese (2005), Apparent polar wander paths for the major continents (200 Ma to the present day): A palaeomagnetic reference frame for global plate tectonic reconstructions, *Geophys. J. Int.*, *163*(2), 727–759, doi:10.1111/j.1365-246X.2005.02638.x.

Schobbenhaus, C., J. H. Gonçalves, J. O. S. Santos, M. B. Abram, R. Leão Neto, G. M. M. de Matos, R. M. Vidotti, M. A. B. Ramos, and J. D. A. Jesus (2004), *Carta Geológica do Brasil ao Milionésimo* [CD-ROM], CPRM, Brazil, ISBN:85-7499-099-4.

Sinito, A. M., D. A. Valencio, and J. F. Vilas (1979), Paleomagnetism of a sequence of upper Paleozoic–lower Mesozoic red beds from Argentina, *Geophys. J.R. Astron. Soc.*, *58*(2), 237–247, doi:10.1111/j.1365-246X.1979.tb01022.x.

Souza, P. A., S. Petri, and R. Dino (2003), Late Carboniferous palynology from the Itararé Subgroup (Paraná Basin) at Araçoiaba da Serra, São Paulo State, Brazil, *Palynology*, *27*, 39–74, doi:10.2113/27.1.39.

Stephens, M. A. (1974), EDF statistics for goodness of fit and some comparisons, *J. Am. Stat. Assoc.*, *69*, 730–737, doi:10.2307/2286009.

Stewart, S. A. (1995), Palaeomagnetic analysis of plunging fold structures: Errors and a simple fold test, *Earth Planet. Sci. Lett.*, *130*(1–4), 57–67, doi:10.1016/0012-821X(94)00251-S.

Tauxe, L. (2002), *Paleomagnetic Principles and Practice*, 299 pp., Springer, New York.

Tauxe, L., and D. V. Kent (2004), A simplified statistical model for the geomagnetic field and the detection of shallow bias in paleomagnetic inclinations: Was the ancient magnetic field dipolar?, in *Timescales of the Paleomagnetic Field*, *Geophys. Monogr. Ser.*, vol. 145, edited by J. E. T. Channell et al., pp. 101–116, AGU, Washington, D. C.

Tomezzoli, R. N. (2001), Further palaeomagnetic results from the Sierras Australes fold and thrust belt, Argentina, *Geophys. J. Int.*, *147*(2), 356–366, doi:10.1046/j.0956-540x.2001.01536.x.

Tomezzoli, R. N., and J. F. Vilas (1999), Palaeomagnetic constraints on the age of deformation of the Sierras Australes thrust and fold belt, Argentina, *Geophys. J. Int.*, *138*(3), 857–870, doi:10.1046/j.1365-246x.1999.00914.x.

Tomezzoli, R. N., R. N. Melchor, and W. D. MacDonald (2006), Tectonic implications of post-folding Permian magnetizations in the Carapacha Basin, La Pampa province, Argentina, *Earth Planets Space*, *58*(10), 1235–1246.

Valencio, D. A., A. C. Rocha-Campos, and I. G. Pacca (1975), Paleomagnetism of some sedimentary rocks of the Tubarão and Passa Dois groups, from the Paraná Basin, Brazil, *Rev. Bras. Geocienc.*, *5*, 186–197.

Van der Voo, R. (1990), The reliability of paleomagnetic data, *Tectonophysics*, *184*(1), 1–9, doi:10.1016/0040-1951(90)90116-P.

Van der Voo, R., and T. H. Torsvik (2001), Evidence for late Paleozoic and Mesozoic non-dipole fields provides an explanation for the Pangea reconstruction problems, *Earth Planet. Sci. Lett.*, *187*(1–2), 71–81, doi:10.1016/S0012-821X(01)00285-0.

Van der Voo, R., and T. H. Torsvik (2004), The quality of the European Permo-Triassic paleopoles and its impact on Pangea reconstructions, in *Timescales of the Paleomagnetic Field*, *Geophys. Monogr. Ser.*, vol. 145, edited by J. E. T. Channell et al., pp. 29–42, AGU, Washington, D. C.

Velázquez, V. F., C. B. Gomes, M. Laurenzi, W. Teixeira, and P. Comin-Chiaramonti (1996), Contribution to the geochronology of the Permo-Triassic alkaline magmatism from the Alto Paraguay Province, *Rev. Bras. Geocienc.*, *26*, 103–108.

Weil, A. B., R. Van der Voo, and B. A. van der Pluijm (2001), Oroclinal bending and evidence against the Pangea megashear: The Cantabria-Asturias arc (northern Spain), *Geology*, *29*(11), 991–994, doi:10.1130/0091-7613(2001)029<0991:OBAEAT>2.0.CO;2.

Zijderveld, J. D. A. (1967), Demagnetization of rocks: Analysis of results, in *Methods and Techniques in Paleomagnetism*, edited by D. W. Collinson, K. M. Creer, and S. K. Runcorn, pp. 254–286, Elsevier, New York.

————————

D. Brandt and M. Ernesto, Department of Geophysics, University of São Paulo, Rua do Matão 1226, 05508-090 São Paulo, Brazil. (daniele@iag.usp.br; marcia@iag.usp.br)

P. R. dos Santos and A. C. Rocha-Campos, Institute of Geosciences, University of São Paulo, Rua do Lago 562, 05508-080 São Paulo, Brazil. (dosantos@usp.br; acrcampo@usp.br)